Semicond. Sci. Technol. **25** (2010) 045019 (6pp) doi:10.1088/0268-1242/25/4/045019

Chemical diffusion in CdTe:Cl

R Grill, B Nahlovskyy, E Belas, M Bugár, P Moravec and P Höschl

Faculty of Mathematics and Physics, Institute of Physics, Charles University, Ke Karlovu 5, Prague 2, CZ-121 16, Czech Republic

E-mail: grill@karlov.mff.cuni.cz

Received 15 October 2009, in final form 11 February 2010
Published 9 March 2010
Online at stacks.iop.org/SST/25/045019

Abstract

High-temperature *in situ* galvanomagnetic measurements are reported in chlorine-doped CdTe, [Cl] $\approx 4 \times 10^{18}$ cm^{-3} at temperatures $T = 600$–$700\,^{\circ}$C near Cd saturation. The chemical diffusion coefficient $\tilde{D}$ is determined by means of relaxation of electrical conductivity after a step-like change of ambient Cd pressure (P_{Cd}) and approximated well by a trial function $\tilde{D}\,(\mathrm{cm}^2\ \mathrm{s}^{-1}) = 1.5 \times 10^7 \exp(-2.55\,\mathrm{eV}/k_bT)/\sqrt{P_{Cd}(\mathrm{atm})}$. Both $\tilde{D}$ and equilibrium conductivity are calculated on the basis of a defect model in which donors Cl_{Te} are compensated by divalent acceptors Cd vacancies (V_{Cd}) and monovalent acceptor complexes ($Cl_{Te}V_{Cd}$). The properties of native point defects are consistent with undoped CdTe. It is shown that $\tilde{D}$ can be fit well assuming different diffusion coefficients for singly and doubly charged V_{Cd}.

1. Introduction

A reliable preparation of x- and gamma-ray CdTe detectors is based on doping by a proper donor element, which compensates native and extrinsic acceptors commonly present in as-grown single crystals. Chlorine substituting Te in the anion sublattice (Cl_{Te}) is often used for this purpose [1, 2]. The research of the defect properties of CdTe:Cl is thus needed to understand the defect structure [3] and to optimize the performance of the detectors. The chemical diffusion affects significantly the material homogeneity and electric properties whenever the material is set out of equilibrium at elevated temperature both during the cooling of as-grown crystal and at the post-growth annealing.

Diffusion of atoms in solids represents a fundamental process affecting the behaviour, properties and practical applicability of the material. The research of diffusion is typically done in two regimes: (i) the isoconcentration diffusion at chemical equilibrium studied using radiotracers, which is known as self-diffusion and characterized by the self-diffusion coefficient D^*, and (ii) the diffusion in a gradient of chemical potential entailing compositional changes, which is named as chemical diffusion or interdiffusion being depicted by the chemical diffusion coefficient $\tilde{D}$. From the mathematical point of view, the former regime (i) is described more easily being ruled by Fick's first and second laws with a typical complementary error function (erfc) or Gaussian-like diffusion profiles [4]. The practical treatment is, however, complicated by difficult manipulation with radioactive materials often hardly accessible or with unappropriate lifetime. The implantation or evaporation of radiotracers breaks the initial isoconcentration profile of monitored species and deviations from single erfc-like profiles are obtained [5, 6]. The latter approach (ii) affords a much wider set of analytical techniques based on electrical, optical and structural changes of the material due to varying composition. The complicated interaction of diffusing species and alternation of dominant diffusion mechanisms in regions with different composition result in anomalous diffusion profiles [7] and request proper generalization of diffusion equations [8]. General reviews on diffusion in solids can be found in [4, 9]. Specialized II–VI semiconductor reviews are given in [10, 11].

The chemical diffusion in CdTe is routinely measured with the time relaxation of electric conductivity as a result of a step-like change of ambient component pressure; the Cd pressure P_{Cd} is used in most cases. Both planar [12] and Hall-bar [13] samples are employed. The convenience of such an approach for CdTe stems from large enough equilibrium densities of dominant (charged) native defects, which are typically close to or above intrinsic carrier density, and well-mastered high-temperature galvanomagnetic measurements. A major part of the research is done on undoped samples; In and Cu doping were used in [14, 15]. An unintentional contamination, however, often appears and the validity of suggested defect and diffusion models is disputed [16]. Consequently, new measurements of $\tilde{D}$ are requested [11]. Though a dependence of $\tilde{D}$ on P_{Cd} or stoichiometry deviation Δ is envisaged

 © 2010 IOP Publishing Ltd Printed in the UK & the USA

[9], the chemical diffusion coefficient of undoped CdTe $\tilde{D}_u$ independent of P_{Cd} was repeatedly found [12, 13]. In doped CdTe no systematic investigation of $\tilde{D}$ versus P_{Cd} is available. For CdTe:Cl no chemical diffusion data are known to us. The radio-tracer diffusion of Cl in CdTe was studied in [6]. In spite of warped diffusion profiles the deduced diffusion coefficient of Cl is ever significantly less than $\tilde{D}$ and the long-range diffusion of Cl can be left out in chemical diffusion simulations.

Following the step change of P_{Cd}, the electrical conductivity relaxation is well approximated by the exponential time dependence characterized by a time constant τ, which correlates directly with the respective chemical diffusion coefficient at final P_{Cd}. It is often observed that τ depends on whether the P_{Cd} step is positive (τ^+) or negative (τ^-). Both $\tau^+ > \tau^-$ and $\tau^+ < \tau^-$ have been noted [11]. In some cases a two-exponential relaxation is ascertained [14]. Factors responsible for such asymmetrical behaviour were discussed in [17] where retarded defect reactions or defect nucleations have been suggested for an explanation.

In this paper we report on the theoretical and experimental study of diffusion in Cl-doped CdTe single crystals with the aim of collecting experimental data, deduce the equilibrium and dynamic properties of relevant point defects and clarify anomalous effects mentioned in the literature. We present a general model describing the ionized defect diffusion including defect reactions and complex formation. Experiments are based on high-temperature *in situ* galvanomagnetic measurements and the conductivity relaxation after the step-like change of ambient Cd pressure. One-dimensional diffusion is assumed throughout the paper being in accord with reported experiments done on planar samples.

2. Theory

2.1. Defect equilibrium

Dominant native point defects routinely assumed in CdTe are the divalent acceptor Cd vacancy V_{Cd}, the divalent donor Cd interstitial Cd_I and the divalent donor Te antisite Te_{Cd} [18, 19]. In Cl-doped CdTe the set of point defects is completed by the shallow donor Cl_{Te} and the shallow acceptor complex called A-centre $A \equiv (Cl_{Te}V_{Cd})$. All defect densities in both neutral and charged modifications are easily calculated with quasi-chemical formalism [20]. In relatively strongly doped CdTe:Cl the Fermi energy μ_F is elevated above the value in undoped CdTe and the density of native donors is reduced. At P_{Cd} near saturation, the equilibrium density of Te_{Cd} is very low and we thus omit this defect in this paper. In analytical calculations we also skip Cd_I and demonstrate the exact numerical results of the validity of such simplification.

The native defect formation, vibration and ionization energies, vibration entropies, factors of degeneracy as well as the gap energy E_g according to [20] are used. The second ionization energy of V_{Cd} set to $E_{v2} = E_v + 0.3E_g$ links charge states of V_{Cd} as

$$\left[V_{Cd}^{2-}\right] = \frac{g_{V_{Cd}^{2-}}}{g_{V_{Cd}^{-}}}\left[V_{Cd}^{-}\right] e^{\frac{\mu_F - E_{v2}}{k_b T}}. \tag{1}$$

The charging of Cl_{Te} is described by the form

$$\left[Cl_{Te}^{+}\right] = \tfrac{1}{2}\left[Cl_{Te}^{0}\right] e^{\frac{E_d - \mu_F}{k_b T}}, \tag{2}$$

with the donor ionization level at $E_d = E_c - 14$ meV [21]. E_v and E_c represent the valence band and conduction band edges, respectively.

The density of Cl-related A-centres formed by singly ionized V_{Cd}^{-} and Cl_{Te}^{+} is calculated with

$$[A^0] = \frac{g_A}{n_o}\left[V_{Cd}^{-}\right]\left[Cl_{Te}^{+}\right] e^{-\frac{E_A}{k_b T}}, \tag{3}$$

$$[A^-] = \frac{g_{V_{Cd}^{2-}}}{g_{V_{Cd}^{-}}}[A^0] e^{\frac{\mu_F - E_a}{k_b T}}, \tag{4}$$

where the configuration degeneracy for the A-centre incorporating donor in the Te sublattice $g_A = 4$, atom density of Cd or Te $n_o = 1.48 \times 10^{22}$ cm^{-3} and the A-centre ionization energy $E_a = E_v + 120$ meV [22]. The A-centre ionization state degeneracies are taken as consistent with V_{Cd} state degeneracies $g_{V_{Cd}^{2-}}/g_{V_{Cd}^{-}} = 1/6$ [23] assuming for simplicity that electronic states in A-centre are localized in the V_{Cd} site and adjacent Cl_{Te}^{+} does not affect their symmetry significantly. E_A is the A-centre formation energy fitted to experimental data.

Having fixed defect thermodynamic parameters, the Fermi energy is calculated by solving the electric neutrality condition

$$n + \left[V_{Cd}^{-}\right] + 2\left[V_{Cd}^{2-}\right] + [A^-] = p + \left[Cd_I^{+}\right] + 2\left[Cd_I^{2+}\right] + \left[Cl_{Te}^{+}\right], \tag{5}$$

where n and p are the free electron and hole densities respectively, with parallel fulfillment of the Cl balance equation

$$[Cl] = \left[Cl_{Te}^{0}\right] + \left[Cl_{Te}^{+}\right] + [A^0] + [A^-]. \tag{6}$$

Leaving out defects with low density Cd_I^{+}, Cd_I^{2+}, A^0 and p in equations (5) and (6) and taking into account equations (1)–(4), both $[A^-]$ and $\left[Cl_{Te}^{+}\right]$ are expressed via [Cl] and n may be expressed as

$$n = [Cl]\frac{1 - \frac{g_A}{n_o}\left[V_{Cd}^{2-}\right] e^{\frac{E_{v2} - E_a - E_A}{k_b T}}}{1 + 2\, e^{\frac{\mu_F - E_d}{k_b T}} + \frac{g_A}{n_o}\left[V_{Cd}^{2-}\right] e^{\frac{E_{v2} - E_a - E_A}{k_b T}}} - 2\left[V_{Cd}^{2-}\right] - \left[V_{Cd}^{-}\right]. \tag{7}$$

Looking for the solution of equation (7), two characteristic regimes are identified in CdTe:Cl. (i) At high P_{Cd} an uncompensated material characterized by $[V_{Cd}] \ll [Cl]$ and stable $n \approx [Cl]$ is obtained. (ii) Lower P_{Cd} results in an increased $[V_{Cd}]$ and mutual donor–acceptor compensation, which allows us to neglect n in equation (7). Moreover, if μ_F deviates from donor and acceptor levels so that

$$e^{\frac{E_{v2}}{k_b T}} \ll e^{\frac{\mu_F}{k_b T}} \ll e^{\frac{E_d}{k_b T}}, \tag{8}$$

the term $2\, e^{\frac{\mu_F - E_d}{k_b T}}$ in the denominator of the fraction and $\left[V_{Cd}^{-}\right]$ may be omitted in equation (7). Such simplification immediately allows us to establish the correlation between μ_F and P_{Cd}:

$$\mu_F \propto \frac{k_b T}{2} \ln P_{Cd}, \tag{9}$$

which yields $n \propto P_{Cd}^{0.5}$ being typical of the compensated CdTe [24]. Relation (9) implies that $\left[V_{Cd}^{2-}\right]$, $[A^-]$ and $\left[Cd_I^{2+}\right]$ are nearly independent of P_{Cd} in compensated regime.

2.2. Chemical diffusion

Given a concentration $[X^q]$ of defect X with a charge q, the flux of X^q along the z direction with the diffusion coefficient D_X^q is expressed by

$$J_X^q = -D_X^q \frac{\partial [X^q]}{\partial z} + \langle v_X^q \rangle [X^q]. \tag{10}$$

The average velocity $\langle v_X^q \rangle$ is specified by an internal electric field induced by the charged defect distribution. Using the Nernst–Einstein relation and basic charge defect statistics, J_X^q can be simplified to the form [8]

$$J_X^q = -D_X^q \frac{[X^q]}{[X^0]} \frac{\partial [X^0]}{\partial z}. \tag{11}$$

The flux of the stoichiometry deviation Δ is equal to

$$J_\Delta = \sum_{X,q} \frac{\partial \Delta}{\partial [X^0]} J_X^q, \tag{12}$$

where

$$\Delta = [\mathrm{Cd}] - [\mathrm{Te}] = \left[\mathrm{Cd}_\mathrm{I}^0\right] + \left[\mathrm{Cd}_\mathrm{I}^+\right] + \left[\mathrm{Cd}_\mathrm{I}^{2+}\right] - \left[\mathrm{V}_\mathrm{Cd}^0\right] - \left[\mathrm{V}_\mathrm{Cd}^-\right] - \left[\mathrm{V}_\mathrm{Cd}^{2-}\right] + \left[\mathrm{Cl}_\mathrm{Te}^0\right] + \left[\mathrm{Cl}_\mathrm{Te}^+\right]. \tag{13}$$

A-centre does not appear in Δ explicitly because it represents both Cd and Te atoms missing in the lattice.

To simplify the calculations, local defect equilibrium and quasi-neutral approximation are used as it is commonly done in such systems [8]. The diffusion of Cl is not assumed. Consequently, all defect densities as well as μ_F may be expressed by means of Cd chemical potential, or Δ, or P_Cd alternatively. Substituting equation (11) into equation (12) and taking into account that $[X^0](z) \equiv [X^0](\Delta(z))$, the chemical diffusion coefficient $\tilde{D}$ is obtained in the form

$$\tilde{D} = -\frac{J_\Delta}{\partial \Delta / \partial z} = \sum_{X,q} D_X^q \frac{[X^q]}{[X^0]} \left| \frac{d[X^0]}{d\Delta} \right|. \tag{14}$$

The partial derivative in equation (12) is simply a sign factor (± 1) to the involved particle fluxes. It manifests in the absolute value of the total derivative in equation (14). Generally, the case would not be so simple, if more complex diffusing species were involved. For example, the involvement of $\mathrm{Te_{Cd}}$ as diffusing defect with $\partial \Delta / \partial \left[\mathrm{Te}_\mathrm{Cd}^0\right] = -2$ would force to fill the 2 in concerned summand in equation (14) as well.

The diffusion flux is usually mediated by native vacancies and interstitials, for that $[X^0] \propto P_\mathrm{Cd}^{\pm 1}$. Equation (14) can then be expressed in the form

$$\tilde{D} = \frac{\sum_{X,q} D_X^q [X^q]}{P_\mathrm{Cd} d\Delta / d P_\mathrm{Cd}}. \tag{15}$$

Applying linear algebra to the set of equations (5), (6) and (13), alternative forms for Δ are obtained:

$$\Delta = [\mathrm{Cl}] + \left[\mathrm{V}_\mathrm{Cd}^{2-}\right] - \left[\mathrm{Cl}_\mathrm{Te}^+\right] + n + \left(\left[\mathrm{Cd}_\mathrm{I}^0\right] - \left[\mathrm{Cd}_\mathrm{I}^{2+}\right] - \left[\mathrm{V}_\mathrm{Cd}^0\right] - [\mathrm{A}^0] - p\right) \tag{16}$$

$$= \tfrac{1}{2}\left\{[\mathrm{Cl}] + \left[\mathrm{Cl}_\mathrm{Te}^0\right] + n - \left[\mathrm{V}_\mathrm{Cd}^-\right] + \left(2\left[\mathrm{Cd}_\mathrm{I}^0\right] + \left[\mathrm{Cd}_\mathrm{I}^+\right] - 2\left[\mathrm{V}_\mathrm{Cd}^0\right] - [\mathrm{A}^0] - p\right)\right\}. \tag{17}$$

In CdTe:Cl the defects collected in parentheses are of low density and can be omitted. The neglected diffusivity of Cl implies that [Cl] remains constant during the whole diffusion process and [Cl] disappears in respective derivatives. Assuming $\mathrm{V}_\mathrm{Cd}^{2-}$ as dominant diffusing entity, $\tilde{D}$ is well approximated with[1]

$$\tilde{D} \doteq \frac{D\left(\mathrm{V}_\mathrm{Cd}^{2-}\right)\left[\mathrm{V}_\mathrm{Cd}^{2-}\right]}{P_\mathrm{Cd} d\left(\left[\mathrm{V}_\mathrm{Cd}^{2-}\right] - \left[\mathrm{Cl}_\mathrm{Te}^+\right] + n\right) / d P_\mathrm{Cd}} \tag{18}$$

$$\doteq \frac{2D\left(\mathrm{V}_\mathrm{Cd}^{2-}\right)\left[\mathrm{V}_\mathrm{Cd}^{2-}\right]}{P_\mathrm{Cd} d\left(\left[\mathrm{Cl}_\mathrm{Te}^0\right] + n - \left[\mathrm{V}_\mathrm{Cd}^-\right]\right) / d P_\mathrm{Cd}} \tag{19}$$

In compensated CdTe:Cl with fulfilled clause (8) $\left[\mathrm{V}_\mathrm{Cd}^-\right]$ may be neglected and both n and $\left[\mathrm{Cl}_\mathrm{Te}^0\right] \propto \mathrm{e}^{\frac{\mu_F}{k_b T}}$. Taking equation (9) into account, $\tilde{D} \propto P_\mathrm{Cd}^{-0.5}$ is predicted for this case.

The model describing chemical diffusion in CdTe:Cl should be consistent with data obtained in undoped CdTe. In undoped CdTe with diffusion driven by both $\mathrm{V_{Cd}}$ and $\mathrm{Cd_I}$ the respective $D\left(\mathrm{V}_\mathrm{Cd}^{2-}\right) = D\left(\mathrm{Cd}_\mathrm{I}^{2+}\right) = \tilde{D}_u/3$ are used [4, 25]. The chemical diffusion coefficient of undoped CdTe [12] is

$$\tilde{D}_u = 5\,\mathrm{e}^{-\frac{1.12\,\mathrm{eV}}{k_b T}}\ \mathrm{cm^2\ s^{-1}}. \tag{20}$$

3. Experiment

The CdTe:Cl ingot with diameter 10 cm and height 3.5 cm was grown by the vertical gradient freeze method [26] at Cd overpressure 1.2 atm, which was fixed by a small excess of Cd in the ampoule. 6N purity starting elements were used. The chlorine dopant with the density $[\mathrm{Cl}] = 5\times10^{18}\ \mathrm{cm^{-3}}$ was introduced into the melt. The cooling speed during the crystallization process at temperatures 1120–1080 °C was 0.5 °C $\mathrm{h^{-1}}$. The ingot was formed by single-crystalline grains with characteristic dimension of several cm. Samples were cut 1 cm from the end of the ingot, polished and etched to final dimensions $5 \times 5 \times 1.6\ \mathrm{mm^3}$.

In situ electrical measurements of the conductivity were performed by the Van der Pauw method. Four Mo wires were welded into the sample. The welding was done in an argon atmosphere to prevent sample and contact oxidation. Each wire was bent after the welding and put into the quartz capillary tube. No sample holder was needed since Mo wires were hard enough to hold the sample inside the ampoule. The sample was placed together with the cadmium source in a quartz ampoule and sealed. Measurements were performed in a two-zone furnace: one zone controlled the sample temperature and the other the Cd partial pressure.

In a typical measurement cycle the sample was held at a fixed temperature and at an initial $\mathrm{P_{Cd0}}$ until its conductivity (σ_0) was stabilized. After that the cadmium source temperature was step-like changed to obtain a sharp change in $\mathrm{P_{Cd}}$ and

[1] Analogous procedure can also be applied in the case of a donor atom occupying Cd sublattice (X_Cd). The corresponding forms differ from equations (18) and (19) by the replacement of $[\mathrm{Cl}_\mathrm{Te}^0]$ by $[X_\mathrm{Cd}^0]$ and $[\mathrm{Cl}_\mathrm{Te}^+]$ by $[X_\mathrm{Cd}^+]$.

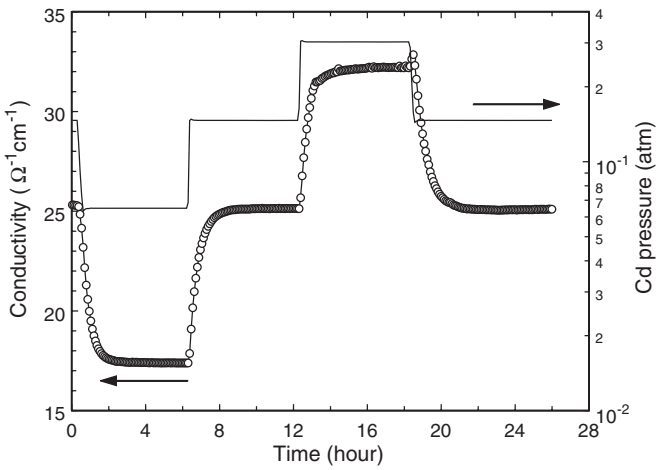

Figure 1. Four steps of conductivity relaxation at 700 °C. A small increase of σ after P_{Cd} step down at 18.2 h is due to the instability of the furnace at the fast cooling of the Cd source. This drawback does not affect the evaluation of $\tilde{D}$, which is determined at a later period of σ_t.

$\tilde{D}$ was established by a single-exponential fit of normalized conductivity relaxation [12, 13]

$$\frac{\sigma_t - \sigma_\infty}{\sigma_0 - \sigma_\infty} = \alpha\, \mathrm{e}^{-\frac{\tilde{D}t\pi^2}{b^2}}, \tag{21}$$

where $b = 1.6$ mm is the sample thickness, σ_∞ is the final conductivity and α is a normalization parameter. In the case of $\tilde{D}(\Delta)$ being dependent on Δ, the fit with equation (21) was applied to the final period of relaxation, when $\Delta(z)$ deviated only weakly from the final Δ.

Measurements at P_{Cd} near Cd saturation were performed with the aim of minimizing the sample sublimation and to prolong the stability of contacts. Three samples were measured, two of them to inspect basic relaxation characteristics and the third sample for detailed measurement of the diffusion. Data of the third sample are presented and evaluated in this paper.

4. Results and discussion

The conductivity relaxation and chemical diffusion have been measured in a relatively narrow temperature interval 600–700 °C. The reason is a large activation energy of diffusion found in this material. Above 700 °C, the relaxation was too fast to stabilize P_{Cd} satisfactorily before the dominant part of relaxation occurred. Below 600 °C, the delay to reach the final state extended up to several days and the setup became unstable during the long delay when several relaxation cycles were measured. A typical profile of σ_t at 700 °C is plotted in figure 1.

Prior to the analysis of $\tilde{D}$ the defect equilibrium according to the theory outlined in section 2.1 was studied. The free carrier and defect densities were calculated solving numerically the set of equations (5) and (6). Due to proximity of μ_F to E_c the degenerate free electron statistics was applied. The conductivity was acquired with electron mobilities $\mu_e(600\,^\circ\mathrm{C}) = 262\,\mathrm{cm}^2\,(\mathrm{V\,s})^{-1}$ and $\mu_e(700\,^\circ\mathrm{C}) = 203\,\mathrm{cm}^2\,(\mathrm{V\,s})^{-1}$ [27].

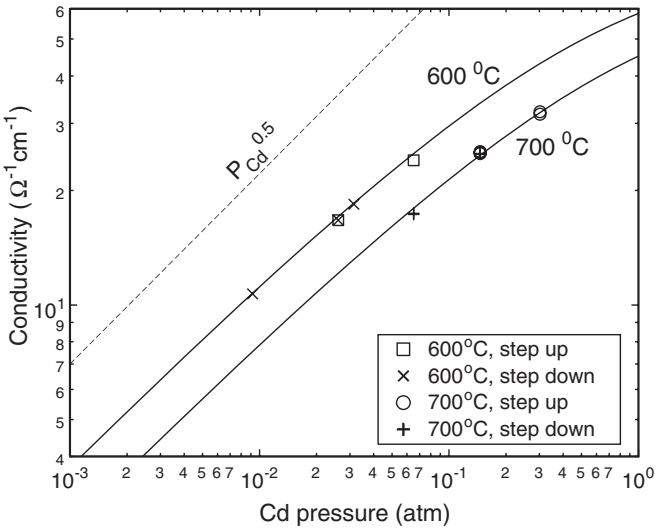

Figure 2. Experimental and theoretical equilibrium conductivity of CdTe:Cl. Remarks 'step up/step down' outline the direction of change of P_{Cd} 'increased/decreased' to reach the final value. The dashed line indicates the slope of $P_{Cd}^{0.5}$ characteristic for a compensated semiconductor.

Measured conductivity and theoretical lines are shown in figure 2. An excellent fit was obtained taking the total Cl density $[\mathrm{Cl}] = 4 \times 10^{18}\,\mathrm{cm}^{-3}$ and the A-centre formation energy $E_A = -0.46$ eV, when other parameters remained unchanged as established in undoped CdTe. The evaluated [Cl] is close to the intentional doping of the melt, which is probably caused by a fast solidification and minimized segregation of Cl into melt. Analogous Cl doping of the melt used in [3] resulted in significantly lower [Cl] found in the solid CdTe:Cl. The fitted E_A is close to $E_A = -0.5$ eV estimated within the Coulomb model [20].

As was mentioned above, $\sigma \propto P_{Cd}^{0.5}$ points to a compensated semiconductor, which slightly converts to an uncompensated material at maximum P_{Cd}. The proximity of σ relaxed after P_{Cd} up/down step proves that there is no effect of the step direction and σ has relaxed into a final state. The detailed view on the defect structure calculated at 700 °C is given in figure 3. It is apparent that in compensated CdTe:Cl the densities of principal point defects change only weakly and $\mathrm{Cl}_{\mathrm{Te}}^{+}$ donors are compensated by A^- and $\mathrm{V}_{\mathrm{Cd}}^{2-}$ acceptors.

The chemical diffusion coefficient was established according equation (21). Several examples of the single-exponential fit of σ_t are plotted in figure 4. It was found that most curves can be easily fit with single exponential, if the initial period of relaxation is skipped. An exception was identified at 700 °C near Cd saturation ($P_{Cd} = 0.3$ atm), where 90% of the relaxation occurred approximately twice faster than the final part used for the determination of $\tilde{D}$. Such a behaviour cannot be explained within a model used here. Taking into account that the effect is apparent only near Cd saturation, we could speculate that partial melting of disturbed regions of the sample, especially along dislocations, might enhance the diffusion there. Similar course of σ_t was reported without relevant comment also in [13]. The theoretical $\tilde{D}$ was calculated via equation (15), where diffusion of both V_{Cd} and Cd_{I} was involved. $D(\mathrm{Cd_I}) = \tilde{D}_u/3$ was used to fit $\tilde{D}_u$ of

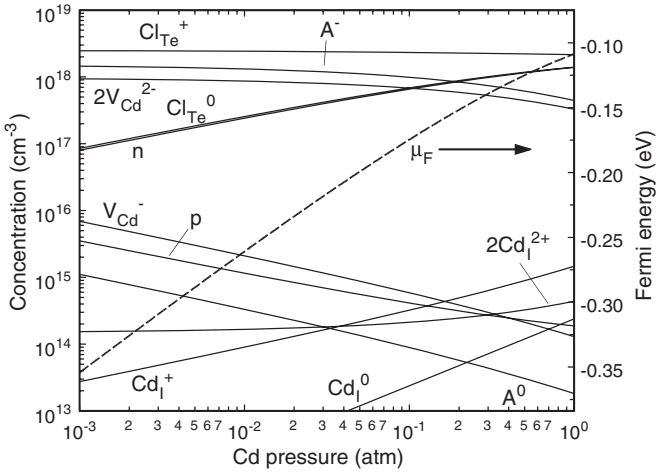

Figure 3. Calculated free carrier and point defect densities of Cl-doped CdTe [Cl] $= 4 \times 10^{18}$ cm^{-3} at 700 °C. The close proximity of n and $[Cl_{Te}^{0}]$ is an accidental effect here. Fermi energy related to the conduction band edge is depicted by the right axis.

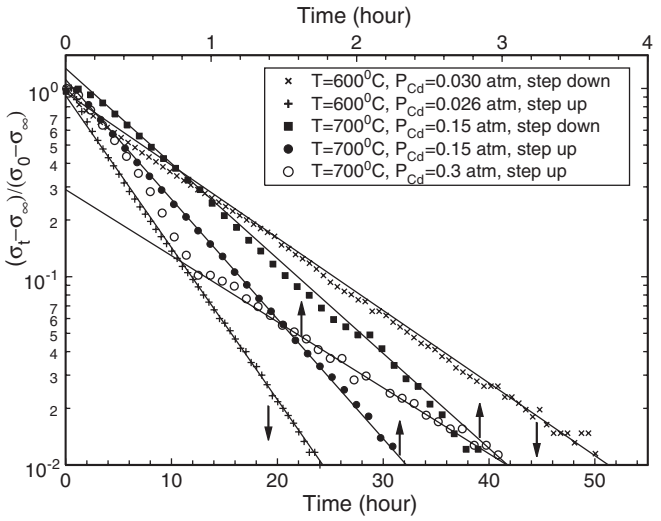

Figure 4. Single-exponential fit of the conductivity relaxation under conditions given in the legend. The time of relaxation at 600 °C/700 °C is depicted by the bottom/upper time axes.

Cd-rich undoped CdTe. $D(V_{Cd}^{2-})$ and $D(V_{Cd}^{-})$ were optimized to describe experimental data both for CdTe:Cl and for Te-enriched undoped CdTe.

The comprehensive summary of experimental and calculated chemical diffusion coefficients is presented in figure 5. Let us pay attention to experimental results at first. Though the scanned interval of P_{Cd} is relatively narrow, it is apparent that $\tilde{D} \propto P_{Cd}^{-0.5}$ as was predicted in equation (19). The relaxation after step up/down yields distinct $\tilde{D}$. This 'memory effect' cannot be explained in standard diffusion theory. We expect that the effect enhances with poorer quality, homogeneity, purity or crystallinity of the material. Comparing with other reports [11] the relaxation time ratio $\tau^{+}/\tau^{-} \approx 0.8$ observed here is insignificant.

Having equilibrium defect properties determined by the fit of conductivity, $\tilde{D}$ was calculated at first according to [25] taking diffusion coefficients of all diffusing native defects equal to $\tilde{D}_u/3$. The point of this approach stems from the

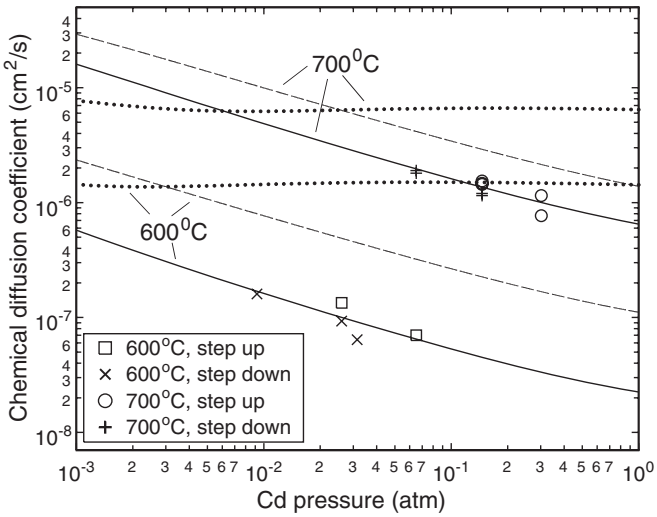

Figure 5. Experimental and theoretical chemical diffusion coefficients at temperatures 600 °C (bottom lines) and 700 °C (upper lines). Dashed lines show $\tilde{D}$ for $D(V_{Cd}^{2-}) = \tilde{D}_u/3$. Full lines depict $\tilde{D}$ for $D(V_{Cd}^{2-})$ and $D(V_{Cd}^{-})$ given by equations (22) and (23). Dotted lines plot $\tilde{D}_u$ of undoped CdTe.

fact that measured $\tilde{D}_u$ in undoped CdTe is independent of P_{Cd} and this choice allows us to accomplish satisfactorily such a result. The respective $\tilde{D}$ is shown in figure 5 by dashed lines. We see that $\tilde{D}$ exhibits predicted slope $\tilde{D} \propto P_{Cd}^{-0.5}$. The magnitude, however, deviates from the values established experimentally. Because V_{Cd}^{2-} is the dominant native defect driving diffusion in CdTe:Cl, the only parameter to be tuned remains $D(V_{Cd}^{2-})$. In parallel, the demand on $\tilde{D}_u$ independent of P_{Cd} can be fulfilled with complementary optimization of $D(V_{Cd}^{-})$. Final fits of $\tilde{D}$ and $\tilde{D}_u$ obtained with

$$D(V_{Cd}^{2-}) = 1.4 \times 10^{3}\, e^{-\frac{1.75\,eV}{k_b T}}\ cm^2\, s^{-1}, \quad (22)$$

$$D(V_{Cd}^{-}) = 2 \times 10^{-5}\ cm^2\, s^{-1}, \quad (23)$$

are plotted in figure 5 by full and dotted lines, respectively. With the aim of characterizing the contribution of different defects to $\tilde{D}$, we decomposed equation (15) into partial summands and show them separately for 700 °C in figure 6. It is apparent that V_{Cd}^{2-} dominates diffusion in CdTe:Cl. Utilization of approximate equation (18) or (19) produces $\tilde{D}$ nearly identical with the full line c in figure 6. In undoped CdTe all defects must be involved to depict $\tilde{D}_u$ properly. Analogous decomposition of $\tilde{D}$ at 600 °C presents similar results as shown in figure 6. Due to peculiar $D(V_{Cd}^{-})$ in equation (23) the effect of V_{Cd}^{-} to the diffusion is more pronounced and reaches up to 30% at minimum $P_{Cd} = 10^{-3}$ atm.

In spite of the completion of all requirements put on the fit and an excellent agreement with the experiment, diffusion coefficients (22) and (23) must be handled cautiously. The $D(V_{Cd}^{2-})$ obtained is in very good agreement with the form evaluated from self-diffusion data [28][2]

$$D(V_{Cd}^{2-}) = \frac{2.74 \times 10^{3}}{f_c}\, e^{-\frac{1.85\,eV}{k_b T}}\ cm^2\, s^{-1}, \quad (24)$$

[2] The validity of a model used for the determination of $D(V_{Cd}^{2-})$ in equation (24) was found to be doubtful in [29].

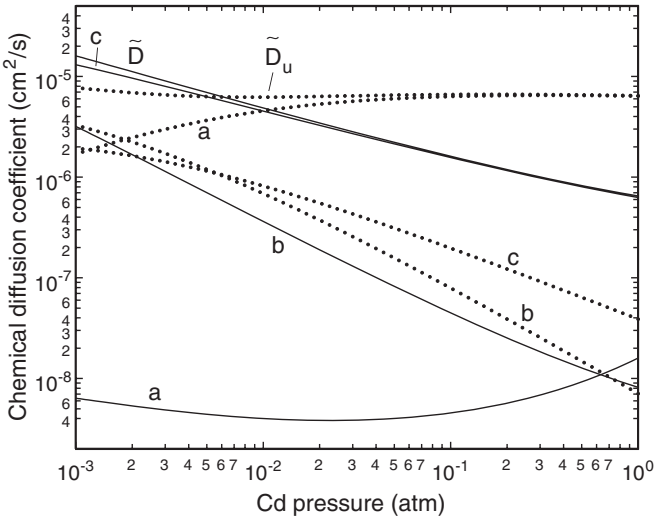

Figure 6. The decomposition of chemical diffusion coefficient of CdTe:Cl (full) and undoped CdTe (dotted) to contributions of different diffusing species at 700 °C. Lines $\tilde{D}$ and $\tilde{D}_u$ are identical with those in figure 5. Lines a, b and c depict diffusion mediated by Cd_I, V_{Cd}^- and V_{Cd}^{2-}, respectively.

where the correlation factor $f_c \approx 1$. Taking into account that equation (24) was not utilized in the calculations, its proximity to equation (22) supports the defect model used. In contrast, the fit of $D\left(V_{Cd}^-\right)$ producing negligible thermal activation looks doubtful and improvements in the model describing chemical diffusion in CdTe should be made.

The numerically established $\tilde{D}$ plotted by full lines in figure 5 is conveniently represented by the form

$$\tilde{D} = \frac{1.5 \times 10^7}{\sqrt{P_{Cd}(\text{atm})}} \, e^{-\frac{2.55\,eV}{k_B T}} \, cm^2\,s^{-1}, \qquad (25)$$

which illustrates the significantly larger activation energy of chemical diffusion 2.55 eV in CdTe:Cl relative to 1.12 eV (equation (20)) found in undoped CdTe.

5. Conclusion

High-temperature *in situ* galvanomagnetic measurements and theoretical calculations based on quasi-chemical formalism were performed in chlorine-doped CdTe, $[Cl] \approx 4 \times 10^{18}$ cm^{-3} at temperatures $T = 600$–$700\,^\circ$C near Cd saturation. The chemical diffusion coefficient $\tilde{D}$ was determined by means of relaxation of electrical conductivity after a step-like change of ambient Cd pressure and described well by a defect model consistent with undoped CdTe in which Cd vacancy proved as a dominant diffusing defect. The diffusion coefficient of V_{Cd}^{2-} agrees well with the previous result deduced from radiotracer diffusion. The evaluated activation energy of the diffusion $E_d = 2.55$ eV is significantly larger than that in undoped CdTe, where $E_{du} = 1.12$ eV. The presented model fits all experimental data on undoped and strongly [Cl]-doped CdTe materials and can be used at least as a good resource for future improvement of models of diffusion in CdTe.

Acknowledgments

This work is a part of the research programme MSM0021620834 financed by the Ministry of Education of the Czech Republic and supported by the Grant Agency of the Czech Republic under contract 202/08/0644.

References

[1] Shoji T, Ohba K, Onabe H, Suehiro T and Hiratate Y 1993 *IEEE Trans. Nucl. Sci.* **40** 405
[2] Popovych V D, Virt I S, Sizov F F, Tetyorkin V V, Tsybrii (Ivasiv), Z F, Darchuk L O, Parfenjuk O A and Ilaschuk M I 2007 *J. Cryst. Growth* **308** 63
[3] Fochuk P, Panchuk O, Shcherbak L and Siffert P 2005 *Phys. Status Solidi* c **2** 1178
[4] Philibert J 1991 *Atom Movements, Diffusion and Mass Transport in Solids* (Les Ulis: Les Éditions de Physique) p 1
[5] Jones E D, Stewart N M and Mullin J B 1993 *J. Cryst. Growth* **130** 6
[6] Jones E D, Malzbender J, Mullin J B and Shaw N 1994 *J. Phys.: Condens. Matter.* **6** 7499
[7] Wolf H, Wagner F and Wichert Th (Isolde Collaboration) 2005 *Phys. Rev. Lett.* **94** 125901
[8] Grill R, Belas E, Bugár M, Höschl P, Nahlovskyy B, Fochuk P, Panchuk O, Bolotnikov A E and James R B 2009 *IEEE Trans. Nucl. Sci.* **56** 1763
[9] Shaw D 1973 *Atomic Diffusion in Semiconductors* ed D Shaw (New York: Plenum) p 1
[10] Shaw D 1992 *Widegap II–VI Compounds for Opto-electronic Applications* (*Electronic Materials* vol 1) ed H E Ruda (London: Chapman and Hall) p 245
[11] Ahmed M U and Jones E D 1994 *EMIS Datareviews Series No 10* ed P Capper (London: INSPEC) p 466
[12] Grill R, Turjanska L, Franc J, Belas E, Turkevych I and Höschl P 2002 *Phys. Status Solidi* b **229** 161
[13] Zanio K 1970 *J. Appl. Phys.* **41** 1935
[14] Rud' Yu V and Sanin K V 1972 *Sov. Phys.—Semicond.* **6** 764
[15] Rud' Yu V and Sanin K V 1974 *Inorg. Mater. USA* **10** 839
[16] Pautrat J L, Francou J M, Magnea N, Molva E and Saminadayar K 1985 *J. Cryst. Growth* **72** 194
[17] Chern S S and Kröger F A 1975 *J. Solid State Chem.* **14** 299
[18] Berding M A 1999 *Phys. Rev.* B **60** 8943
[19] Grill R, Franc J, Höschl P, Turkevych I, Belas E, Moravec P, Fiederle M and Benz K W 2002 *IEEE Trans. Nucl. Sci.* **49** 1270
[20] Grill R, Franc J, Höschl P, Turkevych I, Belas E and Moravec P 2005 *IEEE Trans. Nucl. Sci.* **52** 1925
[21] Schlesinger T E, Toney J E, Yoon H, Lee E Y, Brunett B A, Franks L and James R B 2001 *Mater. Sci. Eng.* **32** 103
[22] Hofmann D M, Omling P and Grimmeiss H G 1992 *Phys. Rev.* B **45** 6247
[23] Berding M A 1999 private communication
[24] Chern S S, Vydyanath H R and Kröger F A 1975 *J. Solid State Chem.* **14** 33
[25] Grill R, Belas E, Franc J, Höschl P and Moravec P 2008 *Nucl. Instrum. Methods* A **591** 218
[26] Höschl P, Ivanov Yu M, Belas E, Franc J, Grill R, Hlídek P, Moravec P, Zvára M, Sitter H and Toth A L 1998 *J. Cryst. Growth* **184/185** 1039
[27] Turkevych I, Grill R, Franc J, Belas E, Höschl P and Moravec P 2002 *Semicond. Sci. Technol.* **17** 1064
[28] Chern S S and Kröger F A 1975 *J. Solid State Chem.* **14** 44
[29] Shaw D 1988 *J. Cryst. Growth* **86** 778